

# **Deciphering the mechanism of myocardial relaxation: The first step to the cure for diastolic dysfunction in heart disease**

Michelle M. Monasky\*

Cardiovascular diseases accounted for 870,000 adult deaths in the U.S. in 2004. More people die of cardiovascular diseases than cancer and AIDS combined in the western world, and this trend is expected to continue. An estimated 5.3 million Americans age 20 and older were in heart failure in 2005 according to the American Heart Association. In the clinic, all patients with congestive heart failure (CHF) present with some degree of diastolic dysfunction<sup>1,2</sup>. Diastolic dysfunction is due to the heart's inability to adequately relax, causing a decrease in stroke volume, and thereby reducing the amount of blood pumped. Current failure to adequately treat diastolic dysfunction is largely due to a lack of understanding about the mechanism of relaxation in myocardium. Thus, it is vital to elucidate the mechanism of myocardial relaxation under normal physiology, to then decipher the malfunction of relaxation in heart failure. The research into the physiological mechanism of relaxation allows us to ultimately understand cardiac relaxation, and strategize hypothesis-driven research that could then be translated to reveal interventional strategies to treat or even cure one of the most devastating diseases in the western world.

An important factor that plays a major role in the contraction and relaxation of myocardium is the amount of tension (diastolic volume/fiber length) that is placed on a muscle. This is analogous to blood filling the ventricle of the heart; the more blood that goes into the ventricle, the more the ventricle has to stretch to accommodate it. There is an intrinsic property

---

\* 304 Hamilton Hall, 1645 Neil Avenue, Columbus, OH 43210. A special thanks to my advisor Dr. Paul Janssen, and also Dr. Jonathan Davis and Mr. Kenny Varian for their help with this project.

of the heart that causes it to contract more forcefully when the cells are at an increased length, or preload. The mechanism behind this intrinsic property remains unclear and is the subject of much research and debate.

Normally, with each heart beat, calcium ions enter the cells of the heart and trigger a release of calcium via an intracellular calcium store (sarcoplasmic reticulum, or SR). These calcium ions travel through the cytosol to the myofilaments, which contain the contractile proteins, of which the main ones are actin and myosin. The calcium binds to troponin-C on the actin myofilament, causing a conformational change of multiple proteins. This change allows myosin to bind to actin, alter their relative position to each other, and thus make the cell contract. The calcium is then partially taken back up into the SR and partially transported out of the cell. During this calcium re-uptake phase, the calcium bound to troponin-C dissociates and the muscle relaxes.

To date a vast majority of the data that relates cardiac relaxation to calcium decline has been either obtained in isolated myocytes where preload and afterload (force against which the muscle contracts; aortic pressure) are generally absent, or under sub-physiological temperature where the rate-limiting steps of relaxation mechanics may greatly differ from those at body temperature. Intact muscles (multicellular preparations called trabeculae; see figure 1) are a more integrated and physiologically relevant model for how the heart as a whole functions, because, unlike individual myocytes, intact muscles contain other aspects of the whole heart such as the extracellular matrix, gap junctions, endothelial cells, and fibroblasts. This integrated preparation thus presents a more physiological setting in which contraction and relaxation can be investigated in vitro. Also, many of the conclusions regarding the relationship between calcium and preload have been elucidated from experiments performed in rats and mice, both of which

have significantly different myosin isoforms and calcium handling properties compared to humans. Given the immense quantitative differences in calcium handling and myofilament isoforms between species, and the significant differences in contractile behavior at room versus body temperature, the role of calcium decline in governing myocardial relaxation remains incompletely understood. Recently, a technique has been developed to follow the intracellular calcium transient that occurs during each beat under near-physiological conditions. This technique uses fluorescent dyes loaded iontophoretically into the cytosol. During this procedure, a fluorescent indicator that binds calcium is introduced into the cell through a micropipette with a miniscule tip (less than 0.1 microns) that penetrates the cellular membrane, and inserts the indicator exclusively into the cytosol where it is trapped. It will then diffuse to other cells via gap junctions. This technique is technically challenging, and used only in a handful of laboratories world-wide. Currently our lab is the only one that has established the assessment of calibrated calcium transients and force of contraction in a higher mammal (rabbit) that possesses similar calcium handling and contractile properties to humans under physiological conditions.

### **Experimental Design:**

Rabbits, whose hearts work much more similarly to humans compared to rats and mice<sup>3</sup>, were used in this study. Briefly, the animals were injected with 5,000 U/kg Heparin and intravenously anesthetized with 50 mg/kg pentobarbital sodium. The chest was opened by bilateral thoracotomy, the heart rapidly excised, and ultra thin trabeculae (see trabeculae muscle photos in figure 1) dissected from the right ventricle. The muscles were placed in a Krebs-Henseleit solution containing (in mM) 137 NaCl, 5 KCl, 1.2 MgSO<sub>4</sub>, 1.2 NaH<sub>2</sub>PO<sub>4</sub>, 20 NaHCO<sub>3</sub>, 10 glucose, and 0.25 CaCl<sub>2</sub>. Twenty mM 2,3-butanedione monoxime (BDM) was added to this solution for the dissection to minimize cutting damage and to arrest the heart<sup>4</sup>. Muscles less than

150  $\mu\text{m}$  thick were mounted into the setup<sup>5-8</sup> and stimulated at 2 Hz while perfused with an oxygenated Krebs-Henseleit solution without BDM, and now containing 1 mM  $\text{Ca}^{2+}$ . The muscles were stretched until an increase in passive (diastolic) force was no longer accompanied by a substantial increase in developed force, and the muscles were allowed about 20 minutes for the force to stabilize. This muscle length corresponds to a sarcomere length of about 2.2  $\mu\text{m}$ , which is about the end-diastolic sarcomere length in the in vivo beating heart<sup>9</sup>.

After the twitch contractions were stabilized, a single myocyte was iontophoretically injected with the fluorescent indicator bis-fura-2, which loads into the cytosol. The use of bis-fura-2 has several advantages. Bis-fura-2 will not cross the cell's membranes because it is charged, which means we can ensure that it will not penetrate and bind to calcium in cellular organelles such as the sarcoplasmic reticulum, mitochondria, or nucleus. Additionally, bis-fura-2 has a high dissociation constant ( $K_d$ ), allowing us to more accurately assess the calcium concentration at both the diastole and systole ends of the transient range. A current of 2-3 nA over a duration of 15-30 minutes at 22°C (to minimize dye leakage) was applied to drive the indicator into the cytosol and to produce a fluorescence well above background levels. After the indicator was loaded, stimulation was turned back on and the bis-fura-2 was given some time to spread to the other myocytes via gap junctions. The temperature was then switched to 37°C and the experiments were begun.

Force-development and simultaneously obtained calcium transients were measured at various extracellular calcium concentrations and muscle lengths (ranging from the muscle being taut to being fully stretched at an optimal length of about 2.2  $\mu\text{m}$ ). At 1.0 mM  $[\text{Ca}^{2+}]_o$ , force and calcium transient amplitude were measured at each of the lengths after stabilization of force. The muscle was then returned to the taut position using the micrometer reading as a guide to assure

accuracy in returning to the exact same length, and  $[Ca^{2+}]_o$  was increased to 2.5 mM. Time was given for the new calcium to circulate throughout the setup, and force and calcium transients were again measured at each of the established lengths. The same procedure was repeated at 4.0 mM  $[Ca^{2+}]_o$ . Twitch contractions were continuously recorded throughout the experiment. Force development was normalized to the cross sectional area of the trabeculae to allow for comparison between muscles of different diameters. Twitches were recorded at each experimental condition upon stabilization of developed tension.

To calibrate each experiment, we obtained an  $R_{min}$  and  $R_{max}$  with solutions containing a calcium chelating agent (EGTA) and high calcium respectively, and used those values together with the published  $K_d$  value for bis-fura-2 (370 nM) to construct a curve of  $Ca^{2+}$  concentration vs. the ratio of 340/380. By using the equation  $[Ca^{2+}]_i = K' [R - R_{min}] / [R_{max} - R]$  where  $K' = 380(\text{no } Ca^{2+}) / 380(\text{max } Ca^{2+}) * K_d$ , we calculated the amount of  $[Ca^{2+}]_i$  that corresponds with our fluorescent ratios.

Data were collected and analyzed using in-house software (LabView, National Instruments). Data were statistically analyzed using t-tests (paired or unpaired) where applicable. Two-way ANOVA with repeated measures followed by a post-hoc t-test was used to determine the influence of the factors “length” and “extracellular calcium concentration” on various dependents (developed force, time from peak tension to 50% relaxation, time from peak calcium to 50% calcium decline, etc.) as well as detect any interaction between the two factors. A two-tailed value of  $P < 0.05$  was considered significant. Data are represented as mean  $\pm$  SEM.

## **Results:**

We set out to measure the effect of length on the intracellular calcium transients. In figure 2, developed force ( $F_{dev}$ ) and intracellular calcium transients at different muscle lengths for a

single twitch can be seen in panels A and B, respectively. These data are normalized in panels C and D. As can be observed, relaxation is significantly prolonged at longer muscle lengths without proportional changes in intracellular calcium amplitude or duration.

The direct relationship between the intracellular calcium transient and developed tension at different muscle lengths is shown in figure 3. Developed tension is higher at longer muscle lengths despite the same intracellular calcium concentration, which demonstrates that in a dynamic state, the relationship between tension development and intracellular calcium transient is not static.

Figure 4 compares developed tension, peak intracellular calcium, time from peak tension to 50% relaxation ( $RT_{50(\text{tension})}$ ), and time from peak calcium to 50% calcium decline ( $RT_{50(\text{calcium})}$ ) changes with increased preload. Comparisons between muscles using t-tests revealed that developed tension is significantly different between each muscle length. Peak intracellular calcium is significantly different between each length except when comparing the two longest lengths ( $P = 0.059$ ). Peak tension to 50% relaxation is significantly different between each muscle length, whereas peak calcium to 50% decline is not prolonged with increasing muscle length. In fact, when comparing the middle length with the longest (t-test,  $P < 0.05$ ) calcium decline actually is faster, in sharp contrast to  $RT_{50(\text{tension})}$ , which progressively slows with increasing length. Calcium transient amplitude increased slightly with an increase in length. Thus, although calcium transient decline does not seem to be a major governing factor in force decline, a governing role of the calcium transient amplitude can not be excluded on the basis of this experiment.

To investigate whether calcium transient amplitude can be a major governing factor on force relaxation, the muscles were exposed to different extracellular calcium concentrations.

Figure 5 shows that both the force of contraction and the calcium transient amplitude are higher when extracellular calcium was increased. However, in panels C and D it can be observed that  $RT_{50(\text{tension})}$  remains the same with different extracellular calcium concentrations ( $P = 0.90$ ), whereas  $RT_{50(\text{calcium})}$  actually decreases with an increase in extracellular calcium ( $P < 0.05$ ). Thus, an increase in  $\text{Ca}^{2+}$  transient amplitude is not responsible for the slow  $RT_{50(\text{tension})}$  decline.

Figure 6A shows the relationship between time from peak tension to 50% relaxation and length. As length is increased, developed force rises while relaxation slows. At a given muscle length,  $RT_{50(\text{tension})}$  is the same despite the differences in force and/or  $[\text{Ca}^{2+}]_o$ . For example, as muscle length was increased at 1.0 mM  $[\text{Ca}^{2+}]_o$ , developed force rose from  $3.1 \pm 0.8$  mN/mm<sup>2</sup> in the taut position to  $23.1 \pm 2.7$  mN/mm<sup>2</sup> when optimally stretched, while  $RT_{50(\text{tension})}$  rose from  $51 \pm 5$  to  $80 \pm 6$  ms at the corresponding lengths. This can be compared to 2.5 mM  $[\text{Ca}^{2+}]_o$ , where developed force rose from  $7.1 \pm 0.9$  mN/mm<sup>2</sup> in the taut position to  $38.9 \pm 4.3$  mN/mm<sup>2</sup> when optimally stretched, while  $RT_{50(\text{tension})}$  rose from  $49.8 \pm 3.4$  to  $83.8 \pm 7.4$  ms at the corresponding lengths. There appears to be a polynomial relationship where force is approaching a maximum as relaxation slows. There may be little or no difference between an  $[\text{Ca}^{2+}]_o$  of 2.5 and 4.0 mM because near-maximal force has already been reached at 2.5 mM  $[\text{Ca}^{2+}]_o$  under the prevailing experimental conditions.

Figure 6B shows the relaxation portion of the twitch relative to the contraction portion of the twitch. At the lowest extracellular calcium concentration and lowest muscle length, a too large signal to noise ratio in the calcium transient prohibited obtaining an  $RT_{90(\text{tension})}$  within acceptable accuracy. Figure 6C demonstrates that the prolongation of  $RT_{50(\text{tension})}$  with length is proportional to the prolongation of  $RT_{90(\text{tension})}$ , and that neither of these parameters are dependent on  $[\text{Ca}^{2+}]_o$ .

Figure 7 shows that the time from peak tension to 50% relaxation slows with increases in muscle length while time from peak to 50% calcium decline is actually accelerated. In addition,  $RT_{50(\text{calcium})}$  accelerates with increases in extracellular calcium concentration while  $RT_{50(\text{tension})}$  does not. Thus, time to 50% relaxation is slower at longer lengths while time for 50% intracellular calcium decline is not prolonged, or even accelerates.

The results of two-way ANOVA, where both muscle length and extracellular calcium concentration were factors, can be seen in table 1. Muscle length was found to be significant for  $RT_{50(\text{tension})}$  and  $RT_{90(\text{tension})}$ , whereas extracellular calcium concentration was not. In summary, the statistical analysis revealed that  $RT_{50(\text{tension})}$  significantly increases with length, but remains unchanged with varying extracellular calcium concentrations when the length remains constant. No prolongation is seen in the rate of intracellular calcium decline at different lengths, but  $RT_{50(\text{tension})}$  slows with increasing length.

### **Discussion:**

This is the first time that length-dependency, or rather the lack thereof, on kinetics of calibrated calcium transients under physiological conditions in a larger mammal are reported. The data from a previous study<sup>10</sup> investigating possible mechanisms of delayed relaxation have been used in many different modeling studies<sup>11-14</sup>. However, in this previous study, the use of small rodents, room temperature, and absence of calcium transient data have not allowed to unambiguously determine the quantitative effects of governing factors of cardiac relaxation under physiological conditions resembling the ones prevailing *in vivo*. The current, more physiologically relevant study will replace the prior one in many modeling studies, and provides the first comprehensive data set of its kind in a larger mammal with a heart that functions similar to a human's.



In the present study, we report that with an increase in muscle length the time course of force relaxation of cardiac muscle dissociates from the intracellular calcium decline. An increase in cardiac muscle length results in a significant increase in relaxation time (slower relaxation), whereas the intracellular calcium decline is virtually unaffected. The results thus show that although it is critical for the calcium concentration to decline for relaxation to take place, the actual duration of relaxation is primarily determined by myofilament properties. While intracellular calcium levels did somewhat increase with increasing length, normalized values revealed that the shape of the calcium transients were the same. Thus, relaxation was significantly prolonged at higher lengths. To further test whether or not this slight increase in calcium transient amplitude may have influenced the time from peak tension to 50% relaxation, we increased the extracellular calcium concentration, which in turn increased the intracellular calcium transient amplitude. A previous study investigated the effect of extracellular calcium concentration on force development and found that there was a smaller percentile change in force when the muscle was stretched at 5.0 mM than at 2.5 mM  $[Ca^{2+}]_o$ , presumably because the muscle's force had reached a max at 2.5 mM  $[Ca^{2+}]_o$ <sup>15</sup>. This is similar to our current study in which the change in developed tension was less between 2.5 mM and 4.0 mM  $[Ca^{2+}]_o$  than when the muscle was stretched than from 1.0 mM to 2.5 mM  $[Ca^{2+}]_o$ . However, in that study cat papillary muscles were stimulated at a sub-physiological frequency of 0.2 Hz. In the present study, developed tension increased at higher extracellular calcium concentrations, but time to 50% relaxation remained the same. Thus, neither an increase in calcium transient amplitude nor speed of calcium decline are primarily responsible for relaxation. This study provides further evidence that myofilament properties, not the rate of calcium decline, mainly regulate force

decline, and thus myofilament properties are governing the rate limiting step(s) in relaxation of adult mammalian myocardium at near physiologic conditions.

In summary, our data provide further insight into the mechanism of myocardial relaxation, and the results show that increasing muscle length significantly dissociates intracellular calcium transient decline from force decline. Before the present study, a conclusive data set comparing simultaneously measured force of contraction and calcium transients was non-existent. Therefore, our physiologically mechanistic approach was necessary to form future hypothesis-driven work directed at the underlying molecular mechanisms. We are known as pioneers in the area of performing experiments under conditions that prevail *in vivo* (i.e. higher species similar to humans, physiological temperature, physiological frequency, pH, intact muscle, applying preload to the muscle, etc.). Our results reveal that myofilament properties, not calcium decline, are the rate-limiting step in myocardial relaxation.

Our future investigations are now aimed at unraveling the pathophysiology behind the mechanism of relaxation of hypertrophic and failing myocardium. This is being done with pulmonary artery banded rabbits with induced right ventricular hypertrophy. First, we will determine what changes occur at the various stages of pathology, from compensatory hypertrophy to end-stage heart failure. We will investigate calcium handling (and mishandling) to determine at which stage the calcium mishandling develops, as well as investigate differences in phosphorylation status of the myofilament proteins<sup>16</sup>. Our results imply that when investigating cardiac relaxation disorders, myofilament properties need to be prominently considered for strategizing future treatment options as they present an under-explored area for pharmaceutical intervention of the most lethal and debilitating disease category in the western world, cardiomyopathies.

## References:

1. Borlaug, B.A. & Kass, D.A. Mechanisms of diastolic dysfunction in heart failure. *Trends Cardiovasc Med* **16**, 273-9 (2006).
2. Satpathy, C., Mishra, T.K., Satpathy, R., Satpathy, H.K. & Barone, E. Diagnosis and management of diastolic dysfunction and heart failure. *Am Fam Physician* **73**, 841-6 (2006).
3. Bers, D.M. Cardiac excitation-contraction coupling. *Nature* **415**, 198-205. (2002).
4. Mulieri, L.A., Hasenfuss, G., Ittleman, F., Blanchard, E.M. & Alpert, N.R. Protection of human left ventricular myocardium from cutting injury with 2,3-butanedione monoxime. *Circ Res* **65**, 1441-9 (1989).
5. Hiranandani, N., Varian, K.D., Monasky, M.M. & Janssen, P.M. Frequency-dependent contractile response of isolated cardiac trabeculae under hypo-, normo-, and hyperthermic conditions. *J Appl Physiol* **100**, 1727-32 (2006).
6. Janssen, P.M.L., Stull, L.B. & Marban, E. Myofilament properties comprise the rate-limiting step for cardiac relaxation at body temperature in the rat. *Am J Physiol Heart Circ Physiol* **282**, H499-H507 (2002).
7. Raman, S., Kelley, M.A. & Janssen, P.M. Effect of muscle dimensions on trabecular contractile performance under physiological conditions. *Pflugers Arch* **451**, 625-30 (2006).
8. ter Keurs, H.E., Rijnsburger, W.H., van Heuningen, R. & Nagelsmit, M.J. Tension development and sarcomere length in rat cardiac trabeculae. Evidence of length-dependent activation. *Circ Res* **46**, 703-14 (1980).
9. Rodriguez, E.K. et al. A method to reconstruct myocardial sarcomere lengths and orientations at transmural sites in beating canine hearts. *Am J Physiol* **263**, H293-306 (1992).
10. Janssen, P.M.L. & Hunter, W.C. Force, not sarcomere length, correlates with prolongation of isosarcometric contraction. *Am J Physiol Heart Circ Physiol* **269**, H676-85 (1995).
11. Hussan, J., de Tombe, P.P. & Rice, J.J. A spatially detailed myofilament model as a basis for large-scale biological simulations. *Ibm Journal of Research and Development* **50**, 583-600 (2006).
12. Schneider, N.S., Shimayoshi, T., Amano, A. & Matsuda, T. Mechanism of the Frank-Starling law - A simulation study with a novel cardiac muscle contraction model that includes titin and troponin I. *Journal of Molecular and Cellular Cardiology* **41**, 522-536 (2006).
13. Niederer, S.A., Hunter, P.J. & Smith, N.P. A quantitative analysis of cardiac myocyte relaxation: A simulation study. *Biophysical Journal* **90**, 1697-1722 (2006).
14. Rice, J.J., Jafri, M.S. & Winslow, R.L. Modeling short-term interval-force relations in cardiac muscle. *American Journal of Physiology-Heart and Circulatory Physiology* **278**, H913-H931 (2000).
15. Parmley, W.W. & Chuck, L. Length-dependent changes in myocardial contractile state. *Am J Physiol* **224**, 1195-9 (1973).
16. Varian, K.D. & Janssen, P.M. Frequency-dependent acceleration of relaxation involves decreased myofilament calcium sensitivity. *Am J Physiol Heart Circ Physiol* **292**, H2212-9 (2007).

**Figure 1. Trabecula dissection and experimental setup.** **A.** Intact rabbit heart. **B.** Inside of the right ventricular free wall. A trabecula highlighted in red. **C.** Trabecula loaded into the experimental setup. The right side is attached to a force transducer, and the left side is attached to a hook. **D.** Trabecula under higher magnification. **E.** Muscle chamber. Perfusion system delivers oxygenated buffer from right to left.

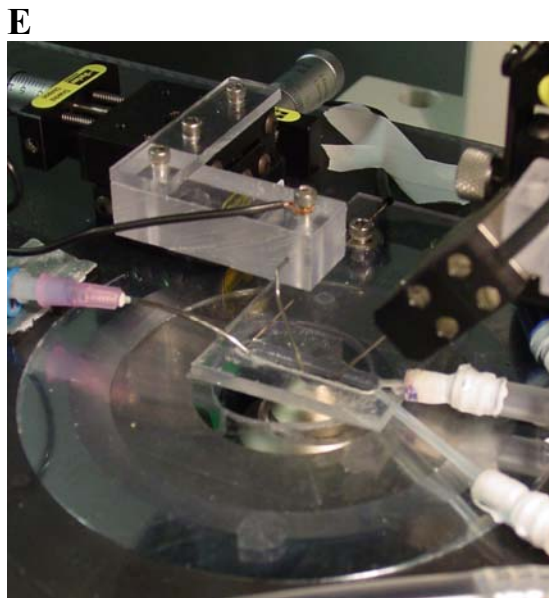
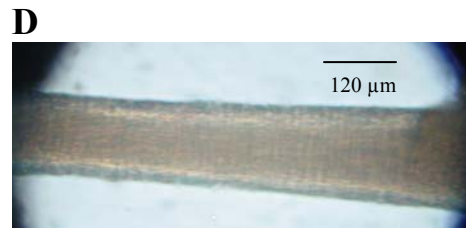
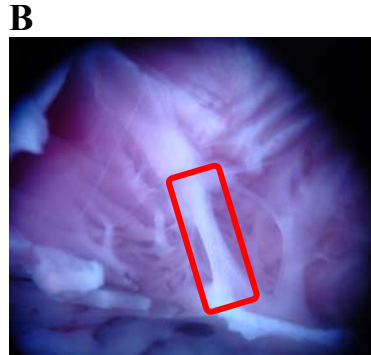
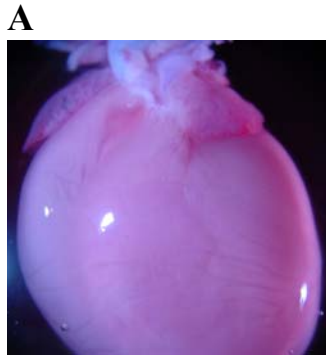


**Figure 2. Effect of muscle length on tension development and  $[Ca^{2+}]_i$ .** Changes in developed force and intracellular calcium transient due to changes in muscle length for a single twitch can be seen in panels A and B respectively. These data are normalized in panels C and D. All data collected at 2 Hz, 2.5 mM  $[Ca^{2+}]_o$ , and at 37°C, n=1 trabecula. Relaxation is prolonged at longer muscle lengths without proportional retention of intracellular calcium. (Experiment date 01/26/07.)

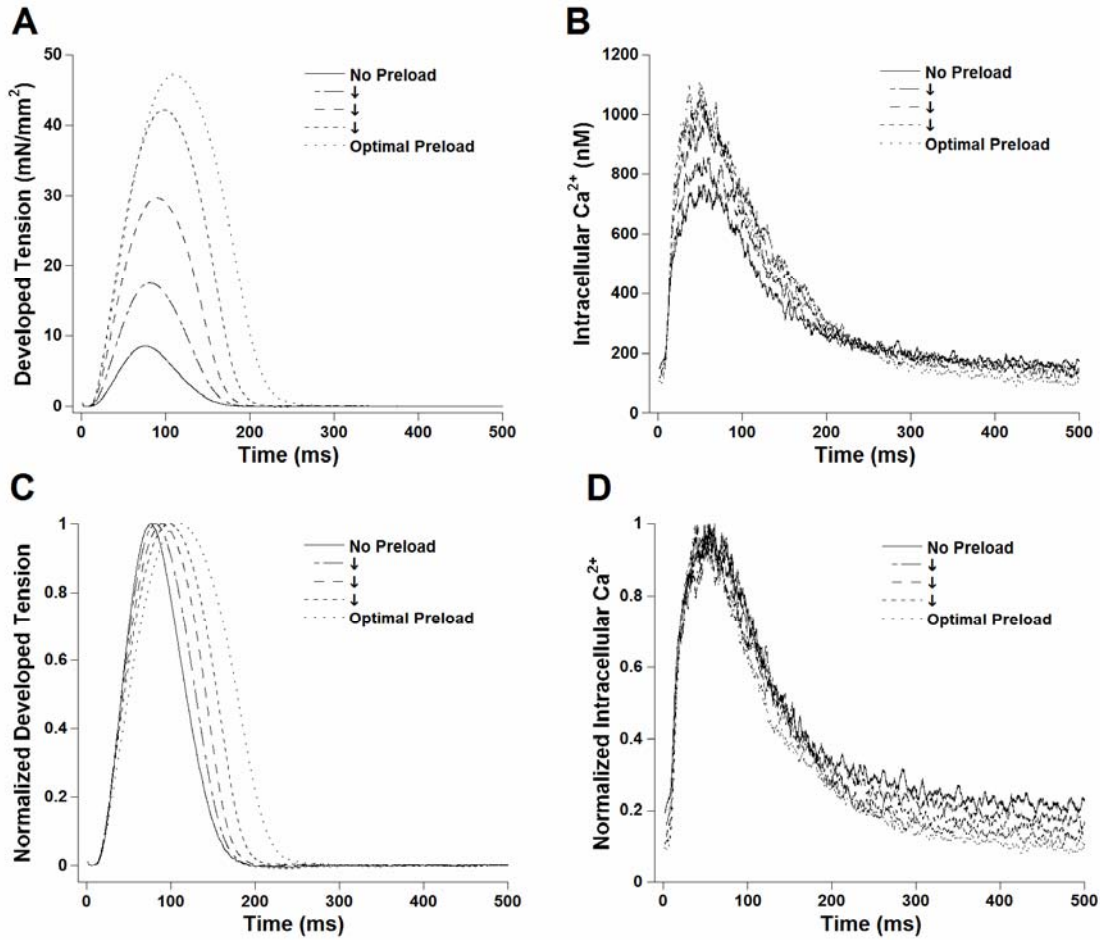


**Figure 3. Developed tension varies with preload despite same  $[Ca^{2+}]_i$ .** These phase plane loops show the relationship between intracellular calcium transient and developed tension at different muscle lengths. Data for developed tension and intracellular calcium concentration were collected simultaneously at 2.5 mM  $[Ca^{2+}]_o$ . Developed tension is higher at longer muscle lengths despite the same intracellular calcium concentration. Data collected at a stimulation rate of 2 Hz, 37 °C, n=1 trabecula. (Experiment date 01/19/07.)

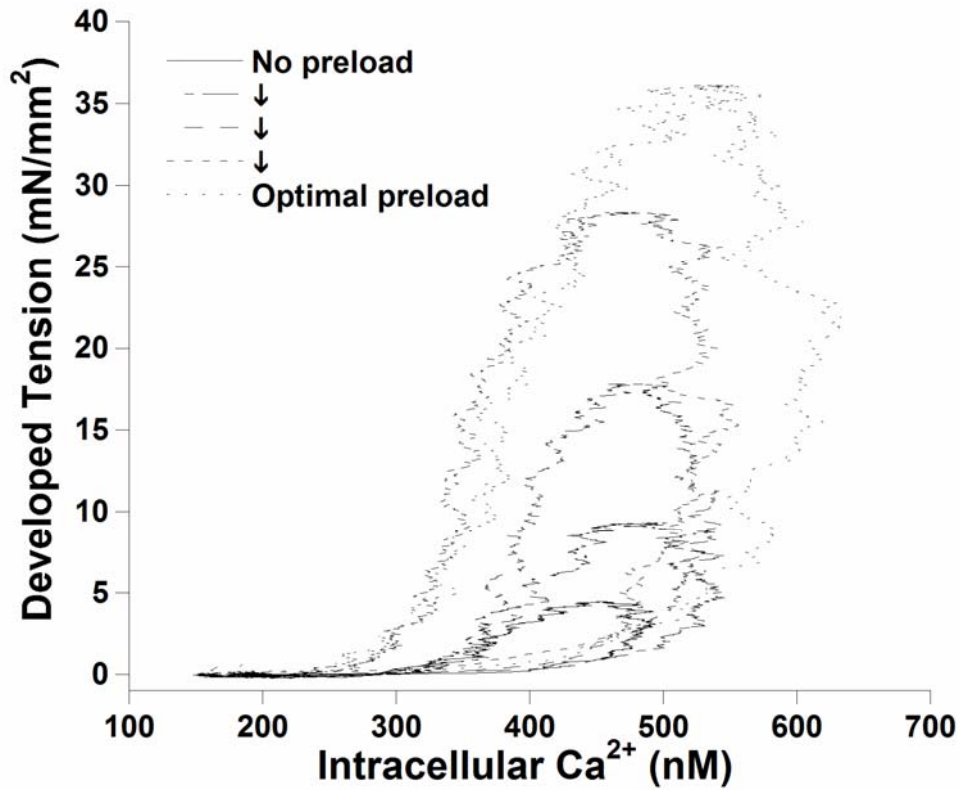


**Figure 4. Tension and  $[Ca^{2+}]_i$  responses to changes in preload.** Developed tension, peak intracellular calcium, peak tension to 50% relaxation, and peak calcium to 50% decline in relation to changes in preload. Data collected at a stimulation rate of 2 Hz, 37 °C, 2.5 mM  $[Ca^{2+}]_o$ , n=8 trabeculae.

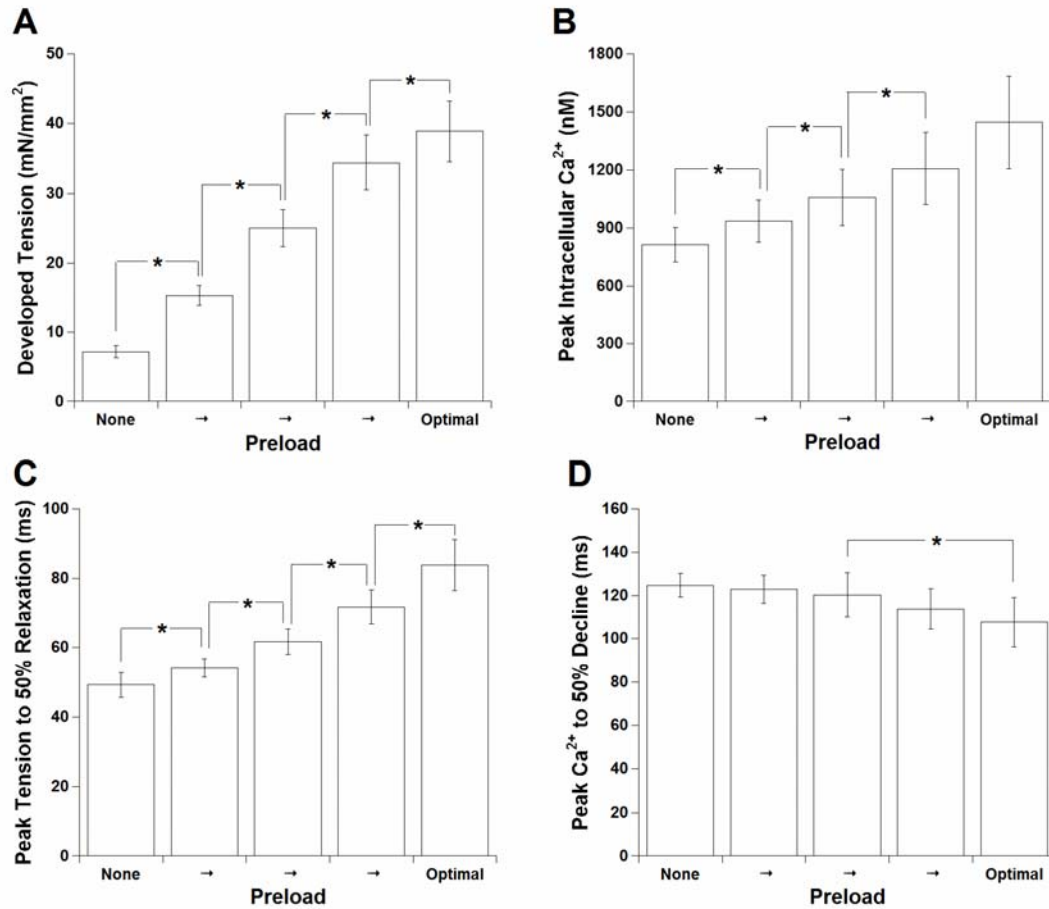


**Figure 5. Tension and  $[Ca^{2+}]_i$  responses to changes in  $[Ca^{2+}]_o$ .** A representative twitch for changes in developed tension and intracellular calcium at three different extracellular calcium concentrations at optimal muscle length can be found in panels A and B respectively (Experiment date 01/26/07.). Changes in peak tension to 50% relaxation and peak calcium to 50% decline in response to changes in extracellular calcium concentration can be seen in panels C and D, respectively. Data collected at stimulation rate of 2 Hz, 37 °C, optimally stretched muscle, n=8 trabeculae.

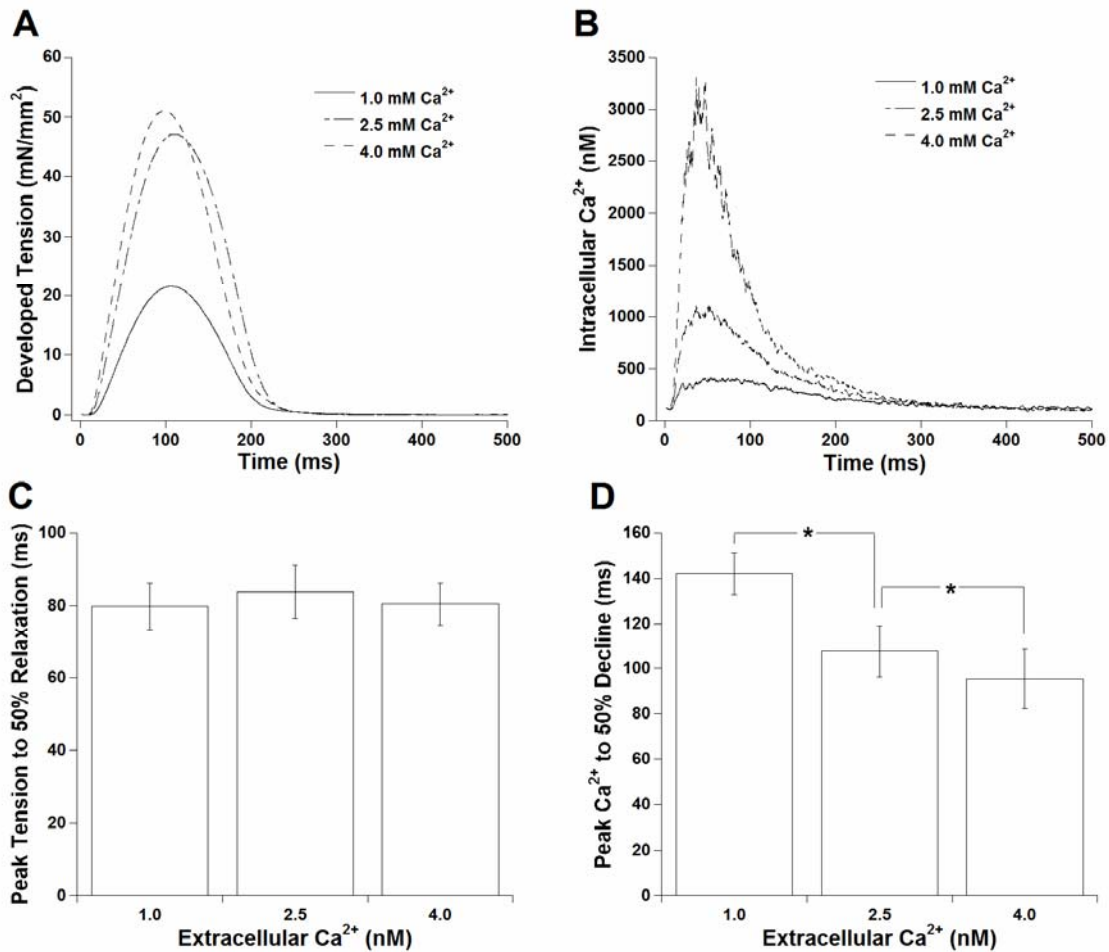




**Figure 6. Tension relaxation the same for corresponding muscle length despite different  $[Ca^{2+}]_o$ .** In panel A, time from peak tension to 50% relaxation changes with length. Panel B shows the first half of the relaxation phase correlates with time to peak contraction, and panel C shows the second phase of relaxation relative to the first. “T” denotes a measurement while the muscle was in the taut position, “S” denotes a measurement while the muscle was optimally stretched, and the remaining points are equally calculated lengths between the taut and optimally stretched positions. Data collected at a stimulation rate of 2 Hz, 37 °C, n=8 trabeculae.

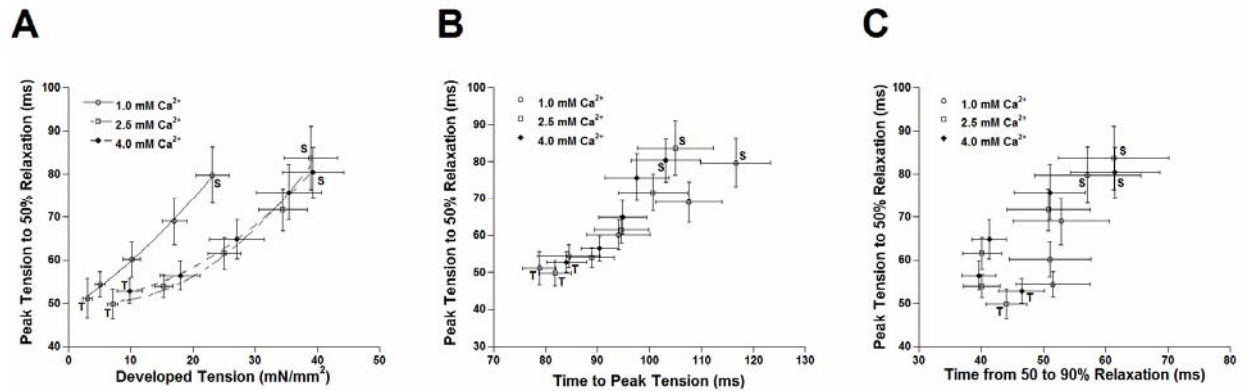


**Figure 7.  $RT_{50(\text{tension})}$  and  $RT_{50(\text{calcium})}$  responses to changes in muscle length.**  $RT_{50(\text{tension})}$  changes significantly with length while  $RT_{50(\text{calcium})}$  does not. “T” denotes a measurement while the muscle was in the taut position, “S” denotes a measurement while the muscle was optimally stretched, and the remaining points are equally calculated lengths between the taut and optimally stretched positions. Data collected at a stimulation rate of 2 Hz, 37 °C, n=8 trabeculae.

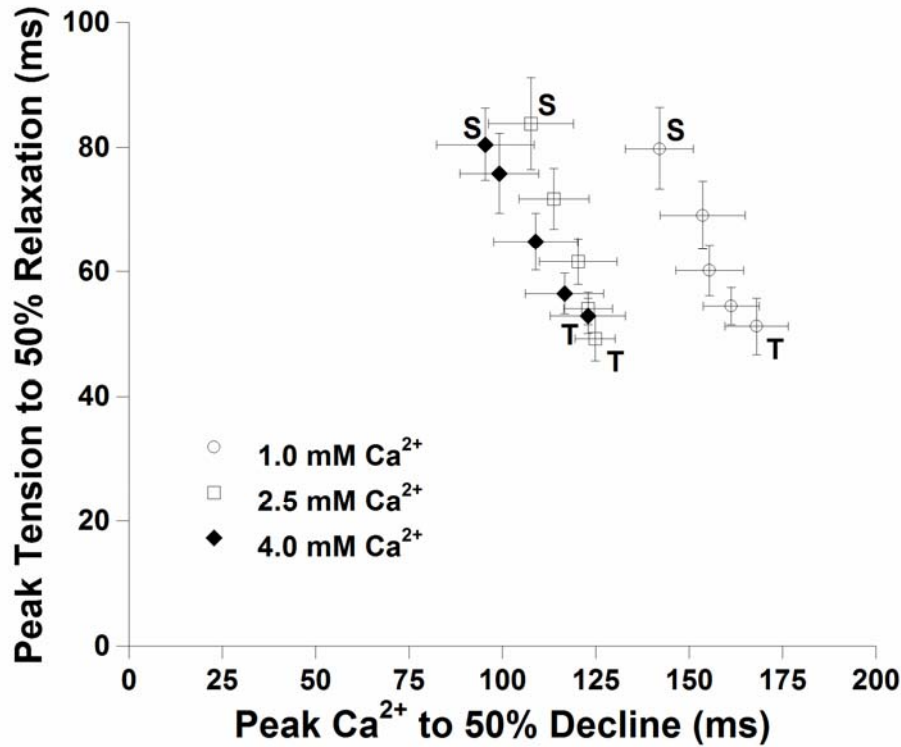


**Table 1. Two-way ANOVA results for various dependents on the factors muscle length and  $[Ca^{2+}]_o$ .** Significant p-values for each of the factors as well as their interaction are marked with an \*. Trends are signified as increasing ( $\uparrow$ ), decreasing ( $\downarrow$ ), or no significant trend (=).

	Muscle Length	$[Ca^{2+}]_o$	Interaction
Developed Tension	$\uparrow$ , < 0.0001*	$\uparrow$ , < 0.0001*	=, 0.52262
$RT_{50(\text{tension})}$	$\uparrow$ , < 0.0001*	=, 0.57922	=, 0.99691
$RT_{90(\text{tension})}$	$\uparrow$ , < 0.0001*	=, 0.59939	=, 0.95142
$RT_{50-90(\text{tension})}$	$\uparrow$ , 0.01464*	=, 0.10755	=, 0.76252
$TTP_{(\text{twitch})}$	$\uparrow$ , < 0.0001*	=, 0.76742	=, 0.66842
$RT_{50(\text{calcium})}$	$\downarrow$ , 0.03544*	$\downarrow$ , < 0.0001*	=, 0.99927
$TTP_{(\text{calcium})}$	$\downarrow$ , 0.03572*	$\downarrow$ , < 0.0001*	=, 0.48248
$Ca^{2+}$ Transient Amplitude	=, 0.0545	$\uparrow$ , 0.00024*	=, 0.43887